Optics and Lasers in Engineering 53 (2014) 79–85

Contents lists available at ScienceDirect

Optics and Lasers in Engineering

journal homepage: www.elsevier.com/locate/optlaseng

Intensity-optimized dithering technique for three-dimensional shape measurement with projector defocusing

Junfei Dai [a], Beiwen Li [b], Song Zhang [b,*]

[a] Mathematics Department, Zhejiang University, Zhejiang 310027, China
[b] Mechanical Engineering Department, Iowa State University, Ames, IA 50011, United States

ARTICLE INFO

Article history:
Received 18 April 2013
Received in revised form
19 July 2013
Accepted 24 August 2013

Keywords:
Fringe analysis
3D shape measurement
Dithering
Optimization
Binary defocusing

ABSTRACT

Our previously proposed phase-based optimization method [1] has proven successful in improving the measurement quality when a dithering technique is used. This paper presents an intensity-based optimization method for 3D shape measurement with binary dithering techniques. Both simulations and experiments find that the phase-based optimization method can generate high-quality phase under a given condition, but it is sensitive to the amount of defocusing. In contrast, the proposed intensity-based optimization method can consistently generate high-quality phase with various amounts of defocusing.

1. Introduction

Digital fringe projection (DFP) techniques have been increasingly used for high-quality 3D shape measurement due to their flexibility and accuracy [2,3]. However, it is still challenging to simultaneously achieve both high measurement speed and high accuracy. The major speed bottleneck (typically 120 Hz) typically comes from the 8 bits representation of an ideal sinusoidal pattern, and the accuracy problem typically comes from the projector nonlinearity [2]. To address the challenges of the conventional DFP technique, we recently developed the binary defocusing technique [4], which has successfully made speed breakthroughs [5]. However, the binary defocusing technique is not trouble free: the measurement accuracy is lower and the measurement range is smaller than the DFP technique [6].

Modulation techniques were proposed to improve the fringe quality of the binary defocusing technique, which modulate the binary patterns according to the ideal sinusoidal patterns. These techniques include 1D modulations and 2D modulations. The pulse width modulation (PWM) techniques [7–10] belong to the 1D modulation category. The PWM technique essentially modulates the binary pattern such that the high frequency harmonics can be easily suppressed or eliminated after defocusing. They all achieved better measurement quality compared with the squared binary method. However, these techniques have limited improvements when fringe stripes are wide [11]. Xian and Su [12] proposed a 2D area modulation technique that could generate high-quality fringe patterns if the manufacturing precision is high enough. But this area modulation technique is difficult to be implemented by a DFP system since it requires more precisely manufactured pixels than a digital video projector can provide. We recently proposed another 2D modulation method [13] that locally modulates the pixels so that it is easier to generate an ideal sinusoidal pattern by defocusing the modulated pattern. However, it is not suited for the wide fringe patterns [14].

Dithering, also called halftoning technique, has been studied in the fields of image processing and printing [15]. Various dithering techniques have been proposed over the years including random dithering [16], ordered dithering [17], and error diffusion [18] techniques. Wang and Zhang have demonstrated that the Bayer dithering method could substantially improve the measurement quality even when the fringe stripes are very wide [19]. However, this technique was found to be unsuccessful when fringe stripes are narrow.

Recently, we proposed a phase-based optimization framework to optimize the Bayer-dithering technique when the projector is nearly focused [1]. This method performs optimization in the phase domain by iteratively mutating the status (0 or 1) of a binary pixel. We demonstrated that for both narrow and wide fringe stripes, substantial improvements could be achieved. However, our further study found that this method was not very stable for different amounts of defocusing.

This paper presents an intensity-based optimization method to further improve the dithering technique. This paper also thoroughly compares the phase-based optimization method with the intensity-based optimization method. Since a 3D shape measurement system utilizes digital fringe projection techniques, the phase

* Corresponding author. Tel.: +1 515 294 0723; fax: +1 515 294 3261.
E-mail address: song@iastate.edu (S. Zhang).

0143-8166/$ - see front matter © 2013 Elsevier Ltd. All rights reserved.
http://dx.doi.org/10.1016/j.optlaseng.2013.08.015

quality ultimately determines the measurement quality and thus these two methods are compared in the phase domain. Both simulations and experiments find that the phase-based optimization method is more sensitive to the amount of defocusing, and the intensity-based optimization method can consistently generate high-quality phase with various amounts of defocusing.

Section 2 explains the principle of the phase-shifting algorithm, the dithering technique and the two optimization methods. Section 3 shows the simulation results comparing the two optimization methods. Section 4 presents the experimental results, and finally Section 5 summarizes this paper.

2. Principle

2.1. Bayer dithering technique

Dithering techniques have been developed to convert a higher bit depth into a lower bit depth, and this is analogous to the halftone technique used in printing. There are various dithering techniques, such as simple thresholding, random dithering, patterning dithering, and ordered dithering. Recently, the dithering techniques have been applied to modulate the binary fringe patterns and have succeeded in providing valid results in 3D shape measurement [19,20]. In the study by Wang and Zhang [19] the Bayer-ordered dithering technique was used. This subsection briefly introduces the fundamentals of Bayer-dithering technique, and the proposed optimization method will be presented in the next subsection.

The Bayer dithering technique compares the original image with a 2D grid of thresholds called Bayer kernel, and then the original image is quantized according to the corresponding pixels in the Bayer kernel: if the grayscale value is larger than the kernel, the pixel is turned to 1 (or 255 grayscale value), otherwise to 0. Neighboring pixels do not affect each other. Different kernels can generate completely different dithering effects. Among the kernels used, Bayer has shown that if the sizes of the matrices are 2^N (N is an integer), there is an optimal dither kernel that results in the pattern noise being as high-frequency as possible [17]. The Bayer kernels can be obtained as follows:

$$M_1 = \begin{bmatrix} 0 & 2 \\ 3 & 1 \end{bmatrix}, \tag{1}$$

which is the smallest 2×2 kernel. Larger Bayer kernel can be generated by

$$M_{n+1} = \begin{bmatrix} 4M_n & 4M_n+2U_n \\ 4M_n+3U_n & 4M_n+U_n \end{bmatrix}, \tag{2}$$

where U_n is an $n\times n$ unit matrix.

2.2. Intensity-optimized dithering technique

The binary dithering technique could generate higher quality fringe patterns than the squared binary patterns after projector defocusing. However, it is far from optimal since the dithering techniques essentially apply a matrix to the whole image, and do not take full advantages of the sinusoidal structures of the desired sinusoidal fringe patterns. This paper proposes to optimize the dithering patterns in the intensity domain, i.e., the criteria to evaluate the quality of optimization are the closeness to the ideal sinusoidal structured patterns.

The main framework of this proposed method can be described by the following steps:

- *Step* 1: *Error pixel detection*. Specifically, taking the difference between the ideal sinusoidal pattern and the Gaussian smoothed binary pattern provides the difference map, from which the error pixels are located. Here, an error pixel refers to the pixel that has intensity error above a given threshold.
- *Step 2*: *Error pixel mutation*. The error pixels are mutated to their opposite status (1 s are changed to 0 s and 0 s are changed to 1 s). After mutations, only good mutations are kept. The good mutation means that the intensity root-mean-square (rms) error between the ideal sinusoidal and the Gaussian smoothed pattern is reduced. If the rms error becomes larger, the original pixel status remains.
- *Step* 3: *Iteration*. This whole algorithm needs to be performed iteratively since if one of the pixels is altered, its neighboring pixels would also be affected after Gaussian smoothing. Therefore, after getting the whole pattern, it would go back to the previous step until the algorithm converges. The convergence rule we proposed to use is that the improvement of intensity rms errors for a round of processing is less than 0.01%.
- *Step* 4: *Threshold reduction*. The threshold is reduced to a smaller number and the whole algorithm goes back to Step 1. The whole algorithm stops when the intensity rms error stabilizes after a number of rounds of iterations. We found that it converges very quickly (typically approximately 15 rounds of iterations).
- *Step* 5: *Phase quality evaluation*. The aforementioned three-step phase-shifting algorithm is used to extract the phase and compare with the ideal phase to evaluate the effectiveness of the proposed algorithm.

2.3. Phase-optimized dithering technique

Our previously proposed phase-based optimization algorithm has also demonstrated its success of improving the dithering technique overall under a certain condition [1]. The major framework of the phase-based optimization method is almost the same compared with the intensity-based optimization method presented in Section 2.1. The main difference between these two methods is that the phase-based method optimizes the dithering technique in the phase domain while the intensity-based method optimizes in the intensity domain. In other words, the rms error used in Steps 1–3 of the intensity-based method is now computed in the phase domain.

Fig. 1 shows example patterns before and after applying the optimization algorithms. Fig. 1(a) shows the desired sinusoidal pattern with a fringe pitch, number of pixels per fringe period, of $T=18$ pixels. The Bayer-dithering technique with a kernel size of 8×8 will result in the pattern shown in Fig. 1(b). We then optimized the pattern with the intensity-based algorithm and the phase-based algorithm, Fig. 1(c) and (d) shows the result.

2.4. Three-step phase-shifting algorithm

A simple three-step phase-shifting algorithm with a phase shift of $2\pi/3$ was used to evaluated the proposed optimization algorithm. Three fringe images can be described as

$$I_1(x,y) = I'(x,y)+I''(x,y)\ \cos[\phi-2\pi/3], \tag{3}$$

$$I_2(x,y) = I'(x,y)+I''(x,y)\ \cos[\phi], \tag{4}$$

$$I_3(x,y) = I'(x,y)+I''(x,y)\ \cos[\phi+2\pi/3], \tag{5}$$

where $I'(x,y)$ is the average intensity, $I''(x,y)$ the intensity modulation, and $\phi(x,y)$ the phase to be solved for

$$\phi(x,y) = \tan^{-1}\frac{\sqrt{3}(I_1-I_3)}{2I_2-I_1-I_3}. \tag{6}$$

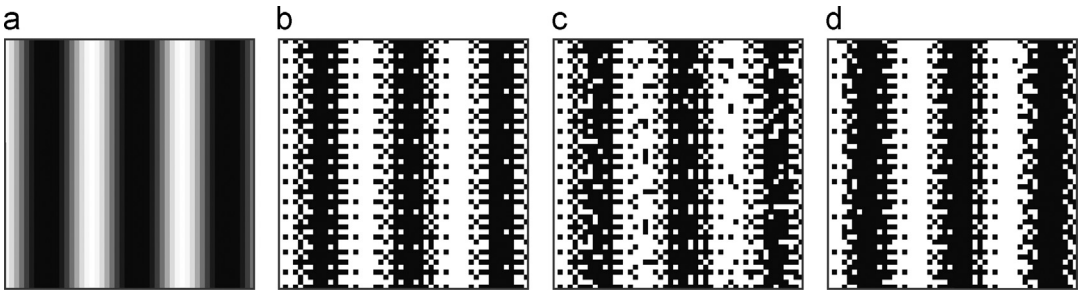

Fig. 1. Example of binary patterns after applying different algorithms. (a) Ideal sinusoidal pattern ($T=18$ pixels); (b) Bayer-dithered pattern of (a); (c) intensity-based optimized pattern; and (d) phase-based optimized pattern.

This equation provides the phase ranging $[-\pi, +\pi)$ with 2π discontinuities. A continuous phase map can be obtained by adopting a spatial or temporal phase unwrapping algorithm. In this research, we used the temporal phase unwrapping method with three frequency phase-shifting algorithms.

3. Simulations

We evaluated the proposed algorithm through simulations where a wide range of fringe stripe breadths was used to ensure that these algorithms could perform well for different practical applications where different densities of fringe pattern could be desired. In this simulation, we used fringe pitches $T=18, 24,\ldots,114, 120$, pixels. The fringe pattern resolution 800×600 to match the projector was used in our experiments (will be discussed in Section 4).

Fig. 2 illustrates the optimization process for a fringe pitch of $T=18$ pixels. We used a very small Gaussian filter (size: 5×5 pixels and standard deviation 5/3 pixels) to evaluate the phase rms error after each iteration. The very small Gaussian filter was used to emulate the nearly focused projector. The phase error is determined by comparing against the ideal phase generated by ideal sinusoidal fringe patterns. Fig. 2(a) shows the results after approximately 15 rounds of iterations with the intensity-based and the phase-based optimization method, where 0 iteration means the starting point where all patterns are the original Bayer-dithered patterns. Compared with the Bayer-dithered patterns, both optimization methods can drastically reduce the phase rms errors. This figure also indicates that after around 10 iterations, both algorithms stabilized. In this research, we used 15 rounds of iterations for all pattern optimizations to ensure the algorithms converge. One may also notice that the phase-based optimization performs better than the intensity-based method for this evaluation condition: Gaussian filter size is 5×5 pixels and standard deviation 5/3 pixels. Furthermore, one may observe that for the intensity-based optimization method, the phase rms error slightly increases after a number of iterations. This is because the method optimizes the patterns in the intensity domain before they are evaluated in the phase domain. Fig. 2(b) illustrates the intensity rms errors for each iteration. As expected, for the intensity-based optimization method, the intensity rms error reduces with the increased number of iterations, and then stabilizes. However, for the phase-based optimization method, the intensity differences actually increase after optimization, which is completely unexpected.

We further evaluated the performance of these two types of optimization methods by changing the amounts of defocusing. In simulation, different sizes of Gaussian filters were applied for the optimized patterns under the filter size of 5×5 pixels with the standard deviation of 5/3 pixels. Fig. 3 shows the results using three different sizes of Gaussian filters for different optimization algorithms. Under the optimization condition (filter size of 5×5 pixels), Fig. 3(a) shows that the phase-based optimization method always performs better than the intensity-based method, which is also indicated by the example shown in Fig. 2(a). However, when the filter size was changed to 9×9 pixels (standard deviation of 9/3 pixels) or 13×13 pixels (standard deviation of 13/3 pixels) meaning that the projector is more defocused, as illustrated in Fig. 3(b) and (c), the performance of the phase-based optimization method, surprisingly, deteriorates rather than improves especially when fringe stripes are narrow (e.g., $T=18$ pixels). The performance was even worse than the original Bayer-dithered pattern, making it difficult to understand. On the contrast, the intensity-based optimization method steadily improves with increased filter size, as expected.

To understand the behavior of the phase-based optimization method, Fig. 3(d)–(f) shows cross sections of the optimized patterns after applying different sizes of Gaussian filters. It can be seen that the phase-based optimized pattern ($T=18$ pixels) is not sinusoidal, the larger the filter size applied, the large the deviation appears to be away from ideal sinusoidal. On the contrast, the intensity-based optimized pattern (again $T=18$ pixels) becomes closer and closer to ideal sinusoidal patterns with the increased size of filters. This explains that the phase-based method cannot consistently perform well with different amounts of defocusing.

We believe that the cause of the unstable problem of the phase-based optimization method is that we applied a three-step phase-shifting algorithm to determine the phase. For a three-step phase-shifting algorithm, the intensity does not need to be ideal sinusoidal to obtain the ideal phase [11]. This is because, as indicated in Eq. (6), if the intensity of three patterns proportionally changes, the phase does not change. This means that a pixel deviates from the ideal sinusoidal curve, but it somehow maintains the proportional relationship for three patterns, the phase will be regarded as optimized, and no further mutations should occur.

4. Experiments

The simulation shows that the intensity-based optimization method has more practical value than the phase-based optimization method in the 3D shape measurement field since the amount of defocusing is difficult to be precisely controlled to the optimization condition. Experiments were also carried out to further evaluate their performance. We utilized a previously developed 3D shape measurement to perform all the experiments. The hardware system includes a digital-light-processing (DLP) projector (Samsung SP-P310MEMX) and a charge-coupled-device (CCD) camera (Jai Pulnix TM-6740CL). The camera was attached with a 16 mm focal length Mega-pixel lens (Computar M1614-MP) with F/1.4 to 16C, and was chosen to have a resolution of 640×480 for all experiments.

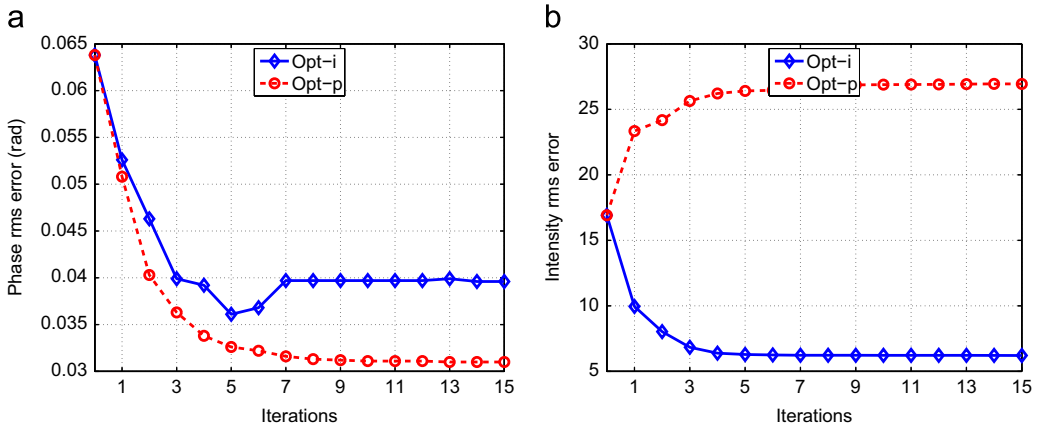

Fig. 2. Comparison between the intensity- and phase-based optimization methods for each iteration. The evaluation was performed by applying a Gaussian filter size of 5×5 pixels and a standard deviation of 5/3 pixels. (a) Phase rms error; (b) Intensity rms error.

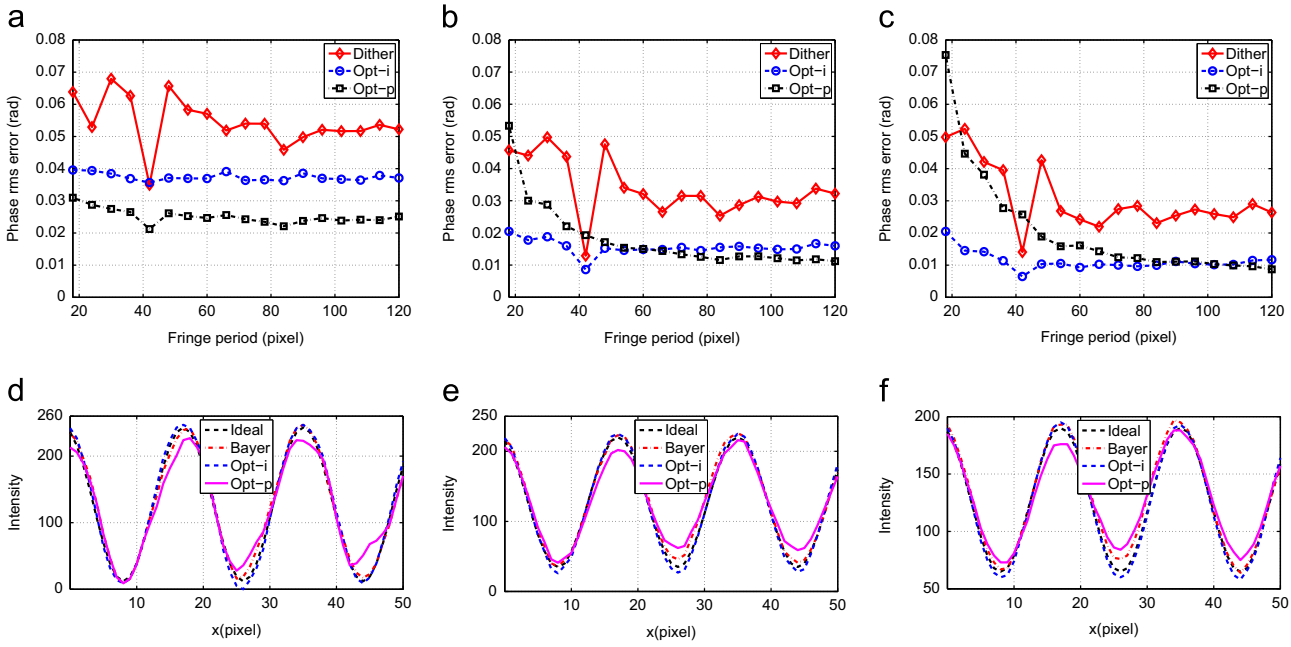

Fig. 3. Performance of the optimized patterns under different amounts of defocusing. (a)–(c) Phase rms errors after applying the 5×5, 9×9, and 13×13 Gaussian filter, respectively; (d)–(f) cross sections after applying the 5×5, 9×9, and 13×13 Gaussian filter, respectively.

The projector has a native resolution of 800×600 with a projection distance of 0.49–2.80 m.

Fig. 4 shows the phase rms error of measuring a uniform flat white board when the projector is defocused to three different levels using the patterns optimized by the phase-based and the intensity-based algorithm. The phase error was computed by taking the difference between the phase obtained from these patterns and the phase obtained by a nine-step phase-shifting algorithm with a fringe period of $T=18$ pixels. Fig. 4(a)–(c) represents three different levels of defocusing used for a standard squared binary patterns with a fringe period of 18 pixels. The projector starts with being nearly focused to being more defocused. Fig. 4(d)–(f) shows the phase rms errors. This experimental results indicate that when the projector is nearly focused, which is similar to our optimization condition (small amount of defocusing), the phase-based method results in smaller phase rms errors, or better phase quality than the intensity-based method. However, if the projector is more defocused, as shown in Fig. 4(e), the intensity-based method starts outperforming the phase-based method in many cases, especially when the fringe period is 18 pixels. Furthermore, Fig. 4(f) shows that if the projector is more defocused, the intensity-based method performs consistently and better than the phase-based method for almost all fringe periods. These experiments further confirm that the intensity-based optimization method indeed can consistently generate high-quality phase while the phase-based method only generate high-quality measurement under a given condition.

We also measured a more complex 3D sculpture to visually compare the differences. Fig. 5 shows the results and Fig. 6 shows the zoom-in views to better visualize the differences. In this experiment, the fringe period we used was $T=18$ pixels. The absolute phase was obtained by a three-frequency phase-shifting algorithm and the temporal phase-unwrapping method whose principle was introduced in Ref. [21]. The other two fringe periods were 21 and 159 pixels. Figs. 5(b)–(d) and 6(a)–(c) show the increased defocusing amounts for the phase-based optimization method. It appears that the phase-based method did not visually improve the quality of measurement when the amount of defocusing

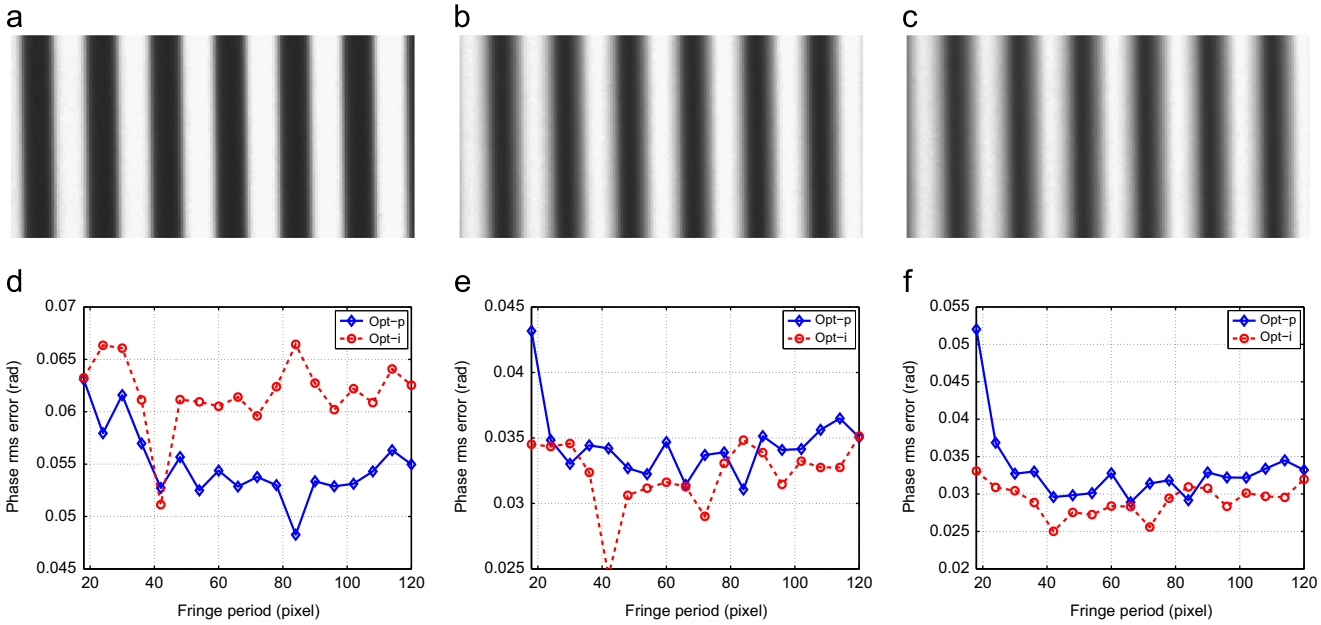

Fig. 4. Experimental results of the optimized patterns under different amounts of defocusing. (a)–(c) Representative squared binary patterns with defocusing level 1 to level 3; (d)–(f) phase rms errors for these three different levels of defocusing using these two optimized fringe patterns with different fringe periods.

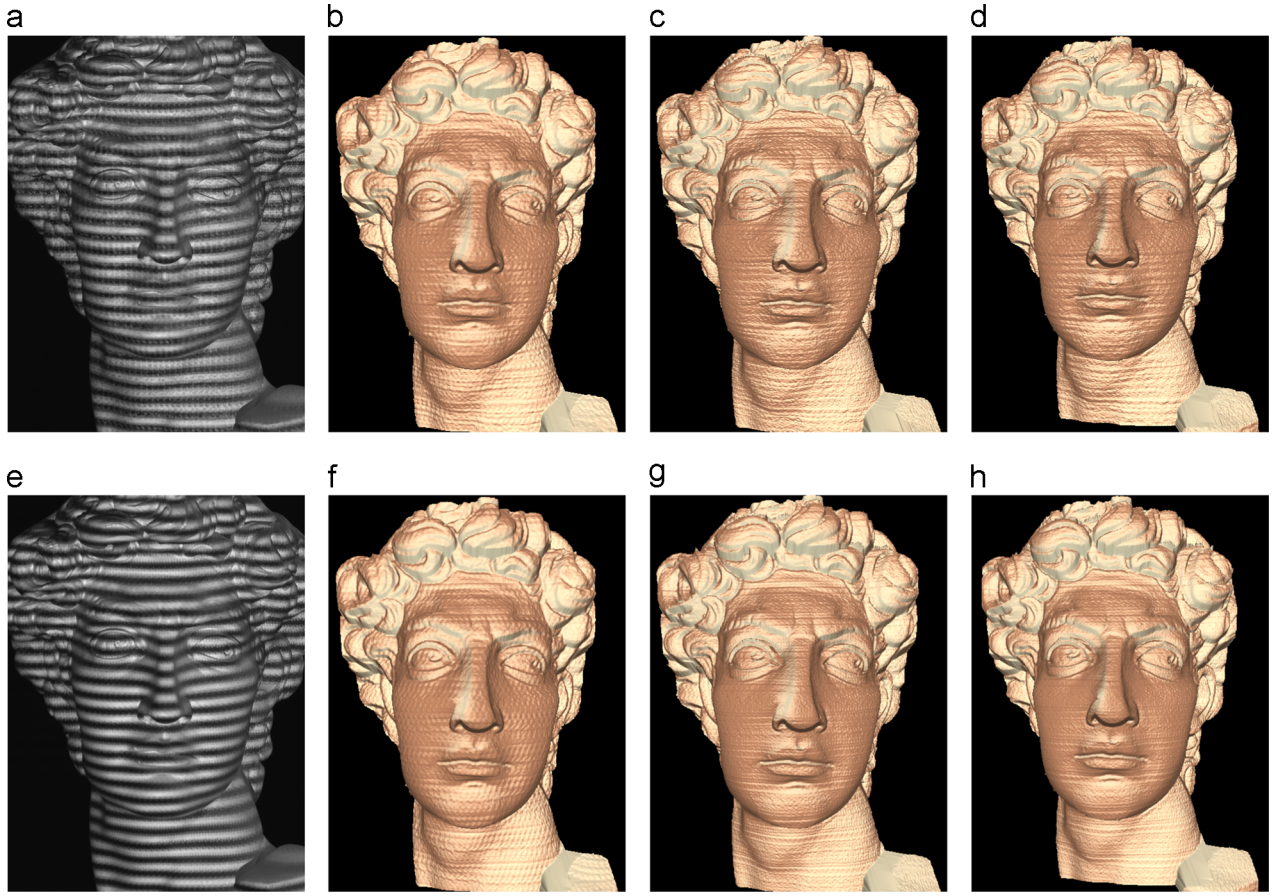

Fig. 5. Measurement results of a complex 3D sculpture. (a) One of the phase-optimized fringe patterns at defocusing level 1; (b)–(d) 3D results using the phase-based optimization method with amount of defocusing level 1 two level 3, respectively; (e) one of the intensity-optimized fringe patterns at defocusing level 1; (f)–(h) 3D results using the intensity-based optimization method with amount of defocusing level 1 to level 3, respectively.

was increased. As a comparison, the results, as illustrated in Figs. 5 (f)–(h) and 6(d)–(f), from the intensity-based optimization patterns are improved when the projector defocusing amount is increased. Even though when the projector is nearly focused, the result from the phase-based optimized method appears slightly better than the intensity-based optimization method, overall, the intensity-based

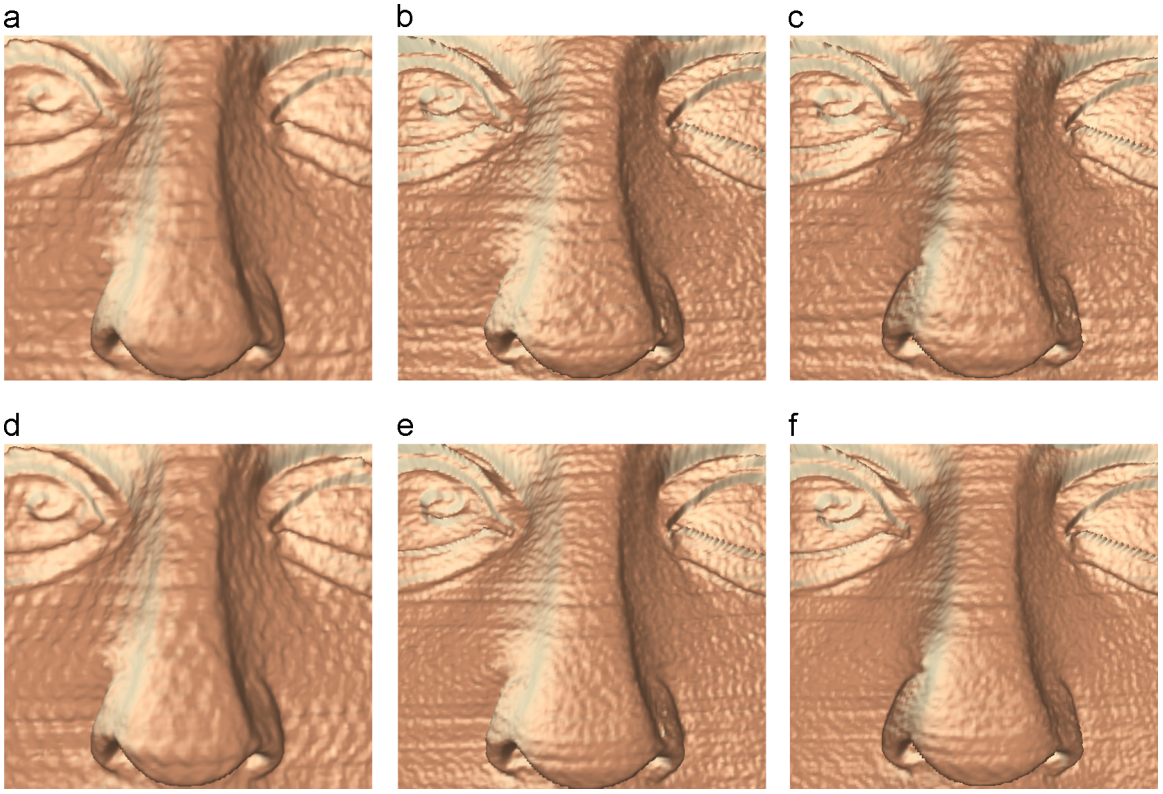

Fig. 6. Close-up view of 3D results shown in Fig. 5. (a)–(c) Zoom-in views of the results shown in Fig. 5(b)–(d), respectively; (d)–(f) zoom-in views of the results shown in Fig. 5(f)–(h), respectively.

optimization method consistently outperforms the phase-based optimization method.

It is important to know that both optimization approaches improved fringe quality when the fringe period is large, and the intensity-based optimization algorithm could improve fringe quality even if the fringe period is small (e.g., 18 pixels). However, our recent study found that if the fringe period is too small (e.g., less than 18 pixels), neither algorithm could perform better than the squared binary method [22]. This is because there are not sufficient number of pixels to operate for the optimization.

5. Conclusion

This paper has presented an intensity-based optimization method to improve the dithering technique for high-quality 3D shape measurement. Compared with the previously proposed phase-based optimization method, the proposed method could more consistently generate high-quality phase under different amounts of defocusing, while the previously proposed phase-based optimization method can perform better only under a certain condition, especially when fringe stripes are narrow. From our simulation and experimental results, it seems that intensity-based optimization method has more practical value than the phase-based optimization method. This is because it is very difficult to precisely control the measurement condition to match the optimal condition requirements of the phase-based method.

Acknowledgment

We would like to thank William Lohry for his time proofreading this paper. This study was sponsored by the National Science Foundation (NSF) under grant numbers CMMI-1150711 and CMMI-1300376.

References

[1] Dai J, Zhang S. Phase-optimized dithering technique for high-quality 3D shape measurement. Opt Laser Eng 2013;51(6):790–5.
[2] Zhang S. Recent progresses on real-time 3-D shape measurement using digital fringe projection techniques. Opt Laser Eng 2010;48(2):149–58.
[3] Geng J. Structured-light 3D surface imaging: a tutorial. Adv Opt Photonics 2011;3(2):128–60.
[4] Lei S, Zhang S. Flexible 3-D shape measurement using projector defocusing. Opt Lett 2009;34(20):3080–2.
[5] Zhang S, van der Weide D, Oliver J. Superfast phase-shifting method for 3-D shape measurement. Opt Express 2010;18(9):9684–9.
[6] Xu Y, Ekstrand L, Dai J, Zhang S. Phase error compensation for three-dimensional shape measurement with projector defocusing. Appl Opt 2011;50(17):2572–81.
[7] Ajubi GA, Ayubi JA, Martino JMD, Ferrari JA. Pulse-width modulation in defocused 3-D fringe projection. Opt Lett 2010;35:3682–4.
[8] Wang Y, Zhang S. Optimum pulse width modulation for sinusoidal fringe generation with projector defocusing. Opt Lett 2010;35(24):4121–3.
[9] Zuo C, Chen Q, Feng S, Feng F, Gu G, Sui X. Optimized pulse width modulation pattern strategy for three-dimensional profilometry with projector defocusing. Appl Opt 2012;51(19):4477–90.
[10] Zuo C, Chen Q, Gu G, Feng S, Feng F, Li R, et al. High-speed three-dimensional shape measurement for dynamic scenes using bi-frequency tripolar pulse-width-modulation fringe projection. Opt Laser Eng 2013;51(8).
[11] Wang Y, Zhang S. Comparison among square binary, sinusoidal pulse width modulation, and optimal pulse width modulation methods for three-dimensional shape measurement. Appl Opt 2012;51(7):861–72.
[12] Xian T, Su X. Area modulation grating for sinusoidal structure illumination on phase-measuring profilometry. Appl Opt 2001;40(8):1201–6.
[13] Lohry W, Zhang S. 3D shape measurement with 2D area modulated binary patterns. Opt Laser Eng 2012;50(7):917–21.
[14] Lohry W, Zhang S. Genetic method to optimize binary dithering technique for high-quality fringe generation. Opt Lett 2013;38(4):540–2.
[15] Schuchman TL. Dither signals and their effect on quantization noise. IEEE Trans Commun Technol 1964;12(4):162–5.
[16] Purgathofer W, Tobler R, Geiler M. Forced random dithering: improved threshold matrices for ordered dithering. IEEE Int Conf Image Process 1994;2:1032–5.
[17] Bayer B. An optimum method for two-level rendition of continuous-tone pictures. IEEE Int Conf Commun 1973;1:11–5.
[18] Kite TD, Evans BL, Bovik AC. Modeling and quality assessment of Halftoning by error diffusion. IEEE Int Conf Image Process 2000;9(5):909–22.

[19] Wang Y, Zhang S. Three-dimensional shape measurement with binary dithered patterns. Appl Opt 2002;51(27):6631–6.
[20] Wang Y, Laughner JI, Efimov IR, Zhang S. 3D absolute shape measurement of live rabbit hearts with a superfast two-frequency phase-shifting technique. Opt Express 2013;21(5):5632–822.
[21] Wang Y, Zhang S. Superfast multifrequency phase-shifting technique with optimal pulse width modulation. Opt Express 2011;19(6):5143–8.
[22] Li B, Wang Y, Dai J, Lohry W, Zhang S. Some recent advances on superfast 3D shape measurement with digital binary defocusing techniques. Opt Laser Eng, doi: http://dx.doi.org.10.1016/j.optlaseng.2013.07.010.